Journal of Hydrology 386 (2010) 27–37

Contents lists available at ScienceDirect

Journal of Hydrology

journal homepage: www.elsevier.com/locate/jhydrol

Advances in ungauged streamflow prediction using artificial neural networks

Lance E. Besaw [a], Donna M. Rizzo [a,*], Paul R. Bierman [b], William R. Hackett [b]

[a] School of Engineering and Mathematical Sciences, University of Vermont, Votey Hall, 33 Colchester Ave., Burlington, VT, USA
[b] Department of Geology, University of Vermont, Delehanty Hall, 180 Colchester Ave., Burlington, VT, USA

ARTICLE INFO

Article history:
Received 18 June 2009
Received in revised form 24 December 2009
Accepted 20 February 2010

This manuscript was handled by
K. Georgakakos, Editor-in-Chief, with the
assistance of Fi-John Chang, Associate Editor

Keywords:
Ungauged streamflow prediction
Artificial neural networks
Time-series analysis
Counterpropagation
Generalized regression neural network

SUMMARY

In this work, we develop and test two artificial neural networks (ANNs) to forecast streamflow in ungauged basins. The model inputs include time-lagged records of precipitation and temperature. In addition, recurrent feedback loops allow the ANN streamflow estimates to be used as model inputs. Publically available climate and US Geological Survey streamflow records from sub-basins in Northern Vermont are used to train and test the methods. Time-series analysis of the climate-flow data provides a transferable and systematic methodology to determine the appropriate number of time-lagged input data. To predict streamflow in an ungauged basin, the recurrent ANNs are trained on climate-flow data from one basin and used to forecast streamflow in a nearby basin with different (more representative) climate inputs. One of the key results of this work, and the reason why time-lagged predictions of steamflow improve forecasts, is these recurrent flow predictions are being driven by time-lagged locally-measured climate data. The successful demonstration of these flow prediction methods with publicly available USGS flow and NCDC climate datasets shows that the ANNs, trained on a climate-discharge record from one basin, prove capable of predicting streamflow in a nearby basin as accurately as in the basin on which they were trained. This suggests that the proposed methods are widely applicable, at least in the humid, temperate climate zones shown in this work. A scaling ratio, based on a relationship between bankfull discharge and basin drainage area, accounts for the change in drainage area from one basin to another. Hourly streamflow predictions were superior to those using daily data for the small streams tested due the loss of critical lag times through upscaling. The ANNs selected in this work always converge, avoid stochastic training algorithms, and are applicable in small ungauged basins.

Introduction

Accurate streamflow forecasts are an important component of watershed planning and sustainable water resource management (Brooks et al., 2003). Streams and rivers modify their channel and overflow their banks during flood events, sometimes inflicting catastrophic damage to human-built infrastructure; conversely riverine ecosystems are often most susceptible during protracted periods of low flow (Allen, 1995). The magnitude and locality of these extreme events can result in degraded surface water quality, loss of agricultural lands, damaged infrastructure, and the mobilization of phosphorus and sediment-related pollutants. Event frequency and severity are exacerbated by climate change and anthropogenic factors (Arnell et al., 2001). Accurate and timely predictions of high and low flow events at any watershed location (either gauged or ungauged) can provide stakeholders the information required to make strategic, informed decisions.

Current methods of forecasting gauged and/or ungauged streamflow fall into four categories: conceptual, metric, physics-based and data-driven. Conceptual models (*e.g.*, MODHYDROLOG) incorporate simplified conceptualizations of hydrological processes (Chiew and McMahon, 1994). Metric models (*e.g.*, IHACRES) do not rely on hydrological features or processes but rather are based on unit hydrograph theory (Jakeman et al., 1990). Physics-based rainfall-runoff models (*e.g.*, InHM) require considerable data and human effort to calibrate, validate, and test but are extremely useful in understanding the governing physics or processes (VanderKwaak and Loague, 2001). Because of the limited resources associated with developing and calibrating conceptual, metric, and physics models (Kokkonen and Jakeman, 2001), data-driven hydrological methods have been widely adopted for forecasting streamflow. Multiple linear regression (MLR), variations of autoregressive moving average (ARMA) models and artificial neural networks (ANNs) are commonly used methods (Wang et al., 2008). Although these data-driven techniques often require similar data as the aforementioned models, they require much less development time, are useful for real-time applications, and prove capable of accurately predicting stream flows (Govindaraju, 2000).

Despite the success of data-driven techniques, the number of ungauged streams greatly compounds the challenges associated with accurately forecasting streamflow. There are over 250,000

* Corresponding author. Tel.: +1 802 656 1495.
E-mail address: drizzo@cems.uvm.edu (D.M. Rizzo).

0022-1694/$ - see front matter © 2010 Elsevier B.V. All rights reserved.
doi:10.1016/j.jhydrol.2010.02.037

rivers in the US, of which less than 25,000 (<10%) are gauged daily by the USGS (Geological Survey, 2009). To accurately predict streamflow in an ungauged basin, streamflow observations must be available nearby. As an example, Mohamoud (2008) combined dominant landscape and climate descriptors from 29 catchments with multiple regression to develop flow duration curves capable of forecasting flow in nearby ungauged basins. We were only able to find one example of ANNs being adopted for forecasting ungauged streamflow (Yang et al., 2007).

In this work, we develop and test a method for predicting ungauged streamflow using two data-driven ANNs and publicly available climate and hydrologic data. A generalized regression neural network (GRNN) and a counterpropagation network (CPN) have been selected because the algorithms always converge, do not require stochastic training, and are applicable to small ungauged basins. Recurrent feedback loops are added to the CPN and GRNN algorithms, allowing future predictions to be based on time-lagged predictions (rather than time-lagged measurements). We use *predicted* flow along with locally-*measured*, time-lagged precipitation and temperature, data as model inputs. Time-series analyses are used to determine the appropriate number of model inputs (*i.e.*, precipitation lagged in time). We compare the GRNN and CPN networks with traditional data-driven methods (MLR and ARMA). We also show the importance of using correctly-scaled climate data by examining the ANN prediction accuracies with data collected on two time scales (daily and hourly). Climate and US Geological Survey streamflow records from sub-basins in Northern Vermont are used for training and testing the methods. Once trained, the predicted flows may be scaled by watershed area to allow for the prediction of streamflow in ungauged basins. To validate flow predictions in ungauged sub-basins, the ANNs are trained on climate-flow data from one sub-basin and used to forecast streamflow in a nearby sub-basin with alternate (nearest, and therefore more representative) climate inputs. Results reveal that predicting with climate data from nearby sub-basins produce accuracies that are not statistically different than those attained when training and predicting in the same sub-basin.

Background

Using an abundance of data from government sources (*e.g.*, US Geological Survey and National Climatic Data Center), data-driven methods are readily applicable and needed to model complex climate-flow relationships in all geographic regions (Walker et al., 2003). Over the past two decades, numerous data-driven ANN algorithms have been used for simulating and forecasting hydrological applications, including feed-forward backpropagation (FFBP) (Govindaraju and Ramachandra, 2000; Chang et al., 2002; Connor et al., 1994), radial basis function (Kisi, 2008; Moradkhani et al., 2004; Singh and Deo, 2007), self-organizing maps (Hsu et al., 1995, 2002), and the adaptive neuro-fuzzy inference system (Chang and Chen, 2001; Chang et al., 2001; Firat, 2008; Firat and Gungor, 2008).

Despite the diversity of ANN algorithms, the multilayer perceptrons (MLP) and the feed-forward backpropagation (FFBP) algorithms are, by far, the most common (accounting for more than 90 of the published applications). Both algorithms have been used to predict streamflow (*e.g.*, Khalil et al., 2005; Maier and Dandy, 2000; Rajurkar et al., 2002; Zealand et al., 1999) and more recently, the FFBP has been shown superior for predicting total sediment load concentration when compared to total sediment transport equations (Emrah et al., 2007), multi-linear regression (Alp and Cigizoglu, 2007; Rajaee et al., 2009), and conventional sediment rating curve models (Rajaee et al., 2009).

Unfortunately, the MLP and FFBP algorithms noted above: (1) require stochastic training, (2) do not always converge (*e.g.*, become trapped in local minima during training), and (3) are widely considered black-box approaches to hydrological modeling (Kingston et al., 2005). These challenges make their application (or transferability to other geographic locations) difficult for users not familiar with ANNs.

To circumvent the above challenges, we focus this research on two ANN algorithms that guarantee convergence (*i.e.*, find the correct weights) and are not stochastic in nature (*i.e.*, do not require iterative training procedures): the counterpropagation network (CPN) and the generalized regression neural network (GRNN). These algorithms have been used in a small number of studies to forecast streamflow (Aytek et al., 2008; Chang and Chen, 2001; Chang et al., 2001). The GRNN was found to outperform FFBP ANN methods when predicting daily (Cigizoglu, 2005a) and monthly streamflow (Cigizoglu, 2005b; Kisi, 2008). However, all previous studies (32 of 33 papers referenced in this manuscript), including those that use CPN and GRNN, use time-lagged flow *measurements* as model inputs. The one notable exception is Wang et al. (2006), who use modified FFBP ANNs to predict streamflow with a 1–10 day lead-time. Using measured streamflow is not suitable for our application, since the end goal is to model discharge in ungauged basins. The use of *predicted* discharge and locally available measured climate data, as model inputs, are key to successfully transferring this technology to ungauged streams.

Other data-driven methods multiple, such as linear regression and time series autoregressive moving average (MLR and ARMA), have been used prevalently throughout the literature for hydrological estimation applications (*e.g.*, Chaloulakou et al. (1999), McKerchar and Delleur (1974) and Yurekli et al. (2005)), streamflow forecasting (*e.g.*, Tangborn and Rasmussen (1976), Phien et al. (1990) and Schilling and Wolter (2005)) and to ANN model evaluation (Hsieh et al., 2003; Adamowski, 2008; Cigizoglu, 2003; Firat, 2008). The autoregressive moving average with exogenous input (ARMAX) models have been extended to incorporate precipitation data to forecast streamflow (Chang and Chen, 2001; Hsu et al., 1995). We use MLR and ARMAX to validate the predictive capabilities of our CPN and GRNN models.

Study site and available data

The Winooski River basin, located in northwestern Vermont, USA, was selected to demonstrate these forecasting algorithms because of the amount of available data (both in space and time) capturing the climate-hydrological relationship of the system. The Winooski basin ($\sim$2700 km^2) has a main branch length of 142 km, originates in the Green Mountains, and receives flow from five major tributaries before discharging into Lake Champlain (Fig. 1). The Mad River, Dog River, Little River, and North Branch and main stem of the Winooski River are all monitored by US Geological Survey (USGS) stream gauging stations, while the Huntington River remains ungauged.

The Winooski basin has a continental or Hemiboreal climate (Koppen classification Dfb), with warm, humid summers and cold winters. The average annual precipitation is about 100 cm (Hijmans et al., 2005). Basin land cover is largely forested in the higher elevations, while moderate development is primarily located in the stream valleys (Albers, 2000; Hackett, 2009). Bedrock is primarily schist and phyllite in the mountains with Cambro-Ordivician siliclastic rocks and carbonates to the west in the Champlain Valley (Doolan, 1996). There is an abundance of low permeability glacial till at elevation, with permeable and impermeable stratified glacial sediments in the valleys, and alluvium near river channels. Unconsolidated cover varies widely throughout the basin, with less material at the higher elevations and more in the valleys.

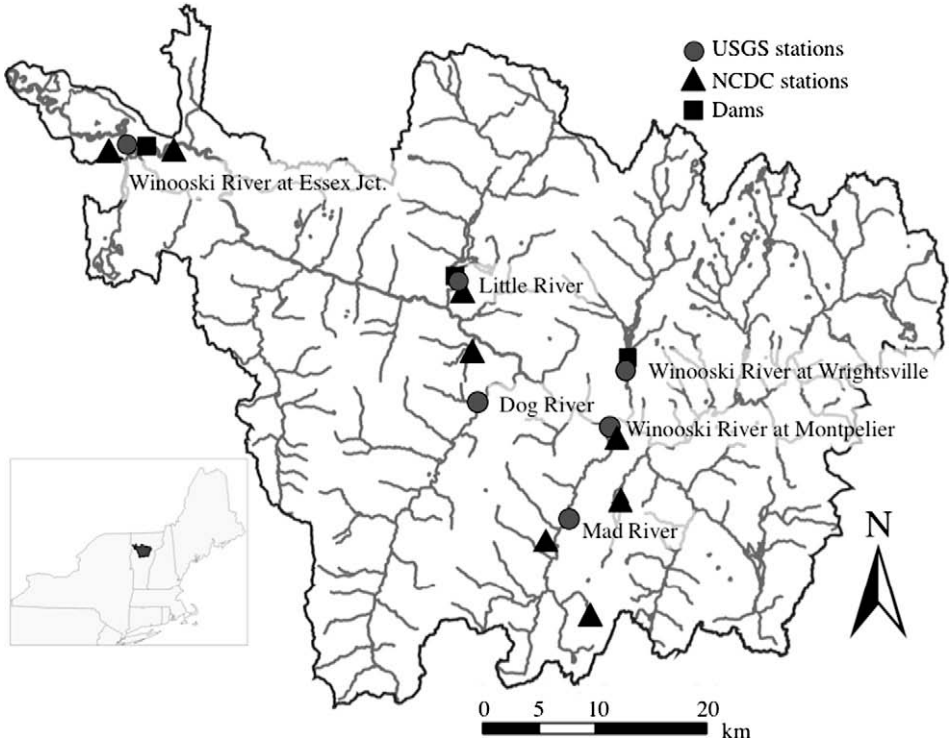

Fig. 1. The Winooski River basin and associated US Geological Survey gauging and National Climatic Data Center weather stations.

Table 1
USGS and NCDC stations within the Winooski River Basin.

Station ID	Description	Elev. (m)	Area (km^2)
USGS 0486000	Winooski River at Montpelier	152	1028
USGS 04285500	Winooski River at Wrightsville	168	179
USGS 04288000	Mad River at Moretown	166	360
USGS 04287000	Dog River at Northfield Falls	184	197
USGS 04290500	Winooski River at Essex Jct.	56	2704
USGS 04289000	Little River at Waterbury	130	287
NCDC 431081	Burlington International Airport	101	–
NCDC 435733	Northfield	204	–
NCDC 435740	Northfield 3	430	–
NCDC 435278	Barre/Montpellier Airport	343	–
NCDC 432843	Essex Junction	104	–
NCDC 438810	Waterbury 2	134	–
NCDC 438815	Waterbury 2 SSE	232	–
NCDC 435273	Montpelier 2	162	–

This study site has hourly and daily streamflow data at six USGS gauging stations and climate data from nine National Climatic Data Center (NCDC) weather stations located within the basin (Table 1). Daily records have captured the climate-hydrologic record of the Winooski River basin since the 1930s. Although temporal cyclicity (including the 7 year NAO cycle) has been observed within the Winooski River basin climate-discharge record (Hackett, 2009), this study focuses on predictions at small enough timescales (days to months) that the impact of such longer-term oscillations is likely negligible.

Methods

Although more than 70 years of flow and climate data exist for this basin, we use daily and hourly data collected only between 1996 and 2006 to train and test our models and avoid non-stationary issues (*e.g.*, we assumed landuse patterns and climate did not change significantly over this time frame). The model output is predicted streamflow. Streamflow, Q (m^3/s), is an average over the entire day of real-time measurements. The model inputs are time-lagged climate data consisting of daily average temperature, T (°C) total precipitation, P (cm/day) and time-lagged estimates of flow, $\hat{Q}$. Since not all sub-basins contain a NCDC weather station, precipitation records associated with the nearest NCDC station are assigned to the USGS stations. Thus, the Dog River USGS gauging station uses the Northfield NCDC precipitation record and the Winooski River at Wrightsville and Montpelier use the Barre/Montpelier Airport NCDC precipitation record. Temperature data from the Burlington International Airport were adjusted for elevation using a lapse rate of 4.1 °C per 1000 m and approximated at the USGS stations. In addition to the daily data, hourly precipitation (cm/h) and streamflow (m^3/s averaged per h) data were gathered for the Dog River basin for this time period.

Data-driven methods require pairs of input–output training data to capture the non-linear, climate-flow relationships. The data are separated into training and prediction sets. Daily and hourly data collected between 1996 and 2006 were used to train and test our models. The 1996–2003 data were used for model training; while data from 2004 to 2006 were used to to make predictions and evaluate the two forecasting methods.

It is common to develop separate ANNs over distinct hydrological seasons to improve forecasts (Singh and Deo, 2007). Thus, we show proof-of-concept using only summer climate-streamflow events (where "summer" is defined as the months from May to October). To reduce training and prediction errors (*e.g.*, predicting flows with missing precipitation record), dates with either missing rainfall or precipitation events (typically days to weeks) have been removed from the record.

Generalized regression neural network (GRNN)

Traditionally, multiple linear regression (MLR) models are the most popular method for predicting streamflow and have the form $\hat{Q} = a_1x_1 + a_2x_2 + \ldots + a_nx_n + \varepsilon$,where $x_1, x_2, \ldots, x_n$ are

the independent input variables (*e.g.*, P, T and measured Q), a_1, $a_2, \ldots, a_n$ are the regression coefficients best fit using a minimum least squares error, ε, between measured and predicted streamflows, denoted $Q(t)$ and $\hat{Q}(t)$ respectively.

Developed as a non-linear, non-parametric extension of MLR, the GRNN is a memory-based network capable of estimating continuous variables (Specht, 1991). A schematic of the daily streamflow prediction model is presented (Fig. 2) to describe the GRNN.

The GRNN consists of four nodal layers: input, pattern, summation, and output. Each layer is fully connected to the adjacent layers by a set of weights (or arcs) between nodes. It is used to regress streamflow, Q, based on a set of input variables, $\mathbf{x}$, defined by some non-linear function $Q = f(\mathbf{x})$, captured by the training data. Training data consist of a set of input vectors, $\mathbf{x}$, and corresponding output: observed flow, Q. In this work we have $I = 7$ input predictor variables, $\mathbf{x}(t) = [P(t-1), \ldots, P(t-4),\ T(t-1),\ \hat{Q}(t-1), \hat{Q}(t-2)]$, while the output is a prediction of daily streamflow. Here $t = 1$ day; however, in some of the test cases we let $t = 1$ h.

The pattern layer has one node for each n training pattern (input–output pairs). The weights on the left side of the pattern nodes store (*e.g.*, are set equal to) the input training vectors, $\mathbf{x}$. Each node in the pattern layer is connected to the two summation layer nodes, S_1 and S_2. The weights linking the pattern layer nodes with summation node S_1 store the streamflows $(Q_1, Q_2, \ldots, Q_n)$ for each input–output training patterns (hence, iterative training is not performed). The weights from the pattern layer nodes to summation node S_2 are set equal to 1.

Once the weights are set, the GRNN may predict $\hat{Q}$. A new input vector for which a prediction is desired, $\mathbf{x}$, is presented to the pattern layer. The Euclidean distance is computed between the input vector and all pattern weight vectors, $\mathbf{w}_i$, where $i = 1,2, \ldots, n$ as: $D_i^2 = (\mathbf{w}_i - \mathbf{x})^T(\mathbf{w}_i - \mathbf{x})$. The distance, D_i^2, is passed to the summation layers and a prediction is computed as:

$$\hat{Q} = \frac{S_1}{S_2} = \frac{\sum_{i=1}^{n} Q_i \exp\left(-\frac{D_i^2}{2\sigma^2}\right)}{\sum_{i=1}^{n} \exp\left(-\frac{D_i^2}{2\sigma^2}\right)},$$

where σ^2 is a smoothing parameter. Large values of σ^2 smooth the regression surface and produce estimates that approach the sample mean; while small values produces a surface with greater chance of discontinuity resulting in nearest neighbor estimates. Intermediate values of σ^2 produce well behaved estimates that approximate the joint probability density function of $\mathbf{x}$ and Q (Specht, 1991). The prediction, $\hat{Q}$, is a weighted average of all stored response observations $(Q_1, Q_2, \ldots, Q_n)$, where each response is weighted exponentially according to its Euclidean distance from input vector $\mathbf{x}_i$. For more details refer to Specht (1991). The GRNN algorithm described in this work was written in MatLab V. 7.4.0.287 (R2007a).

We modified the traditional GRNN architecture to allow for recurrent feedback (dashed line of Fig. 2). These recurrent connections allow recently predicted streamflows $\hat{Q}(t-1), \hat{Q}(t-2), \ldots$ to be passed back to the input layer and used to predict $\hat{Q}(t)$ during the next time step(s). The modification involves adding the time-lagged streamflow into the training input vector, $\mathbf{x} = [x_1, x_2, \ldots, x_m, \hat{Q}(t-1), \ldots]$ and does not change the GRNN algorithm.

Counterpropagation network (CPN)

The relatively simple, yet powerful, counterpropagation algorithm sequentially combines the Kohonen self-organizing map and a Grossberg classification layer (Hecht-Nielsen, 1987). The combination leverages the unsupervised clustering self-organizing map with known output responses (*a priori* categories) to create a statistical mapping between predictor and response vectors (input–output pairs).

The CPN architecture consists of three nodal layers: input, Kohonen and Grossberg (Fig. 3). All nodes in adjacent layers are connected via weights; matrix w_{ij}, where I represents a node in the input layer and j a node in the Kohonen layer, likewise u_{jk} represents the weights linking the J Kohonen and K Grossberg nodes. Like almost all supervised ANNs, the execution of the CPN is defined by a training and prediction phase.

During training, the weights are iteratively adjusted to map the set of input predictor vectors, $\mathbf{x}$, to the set of associated response vectors, $\mathbf{Q}$, defined by some non-linear function $\mathbf{Q} = f(\mathbf{x})$, represented by the training data. A given input vector, $\mathbf{x}$, consisting of I variables $(x_1, x_2, \ldots, x_I)$, is passed to the hidden layer. A similarity metric is computed that compares the input vector with the weight vector, $\mathbf{w}_j$, associated with each of the Kohonen nodes. The Kohonen node with the weight vector most similar to the input vector is identified as the *winning* node; and the weights associated with this winning hidden node are adjusted to be more similar to the input vector by:

$$\Delta\mathbf{w}_j = \begin{cases} \alpha(\mathbf{x} - \mathbf{w}_j), & \text{for } j = \text{winning node}, \\ 0, & \text{for } j \neq \text{winning node}, \end{cases}$$

where α is the Kohonen learning rate ($\alpha = 0.7$ in this work). Through a winner-take-all activation function, the winning Kohonen node propagates $z_{j=winner} = 1$ to the nodes of the Grossberg layer, while all other Kohonen nodes pass $z_{j\neq winner} = 0$. The network output $\hat{Q}$ is computed as $\hat{Q}_k = \sum_{j=1}^{J} u_{jk} z_j$, where z_j is the activation value passed from the jth Kohonen node, u_{jk} is the Grossberg weight connecting the jth Kohonen node and the kth Grossberg node and $\hat{\mathbf{Q}}_k$ is the kth component of the output vector, $\hat{\mathbf{Q}}$. Both the predicted and observed flow vectors are used to adjust the Grossberg weights as:

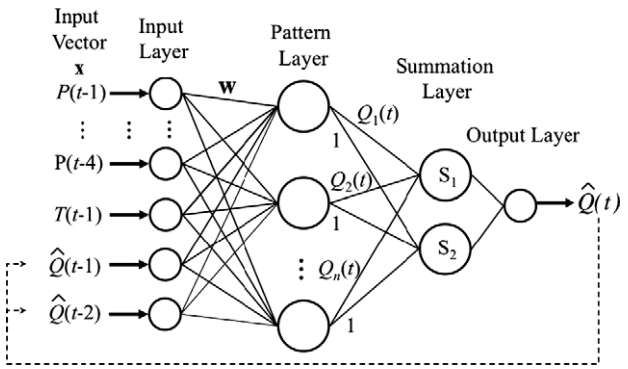

Fig. 2. Architecture for the daily streamflow GRNN with optional recurrent (feedback) connection (dashed arrow).

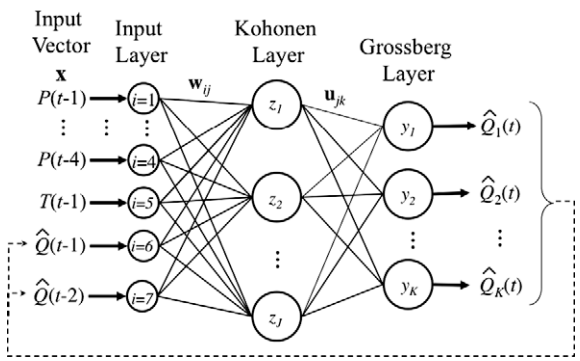

Fig. 3. Architecture of daily streamflow CPN with recurrent (feedback) connection (dashed line).

$$\Delta \mathbf{u}_j = \begin{cases} \beta(\mathbf{Q} - \hat{\mathbf{Q}}), & \text{for } j = \text{winning node}, \\ 0, & \text{for } j \neq \text{winning node}, \end{cases}$$

where β is the Grossberg learning rate ($\beta = 0.1$). This process is repeated for all input–output pairs, until the network has learned the streamflow mapping defined by $\mathbf{Q} = f(\mathbf{x})$ to some user-defined convergence criterion (in this work, a summed root-mean-square error value $<10^{-6}$).

After convergence, the network weights are fixed and the CPN may be used for streamflow prediction. During this prediction phase, input vectors that were not used to train the ANN are presented to the network for prediction. The number of hidden nodes used to generate predictions may be set to one for nearest-means classification or to three for smoother predictions (Besaw and Rizzo, 2007). The latter was used in this work.

Like the recurrent GRNN, the CPN has been modified to incorporate a recurrent feedback loop (dashed lines in Fig. 3) allowing time-lagged predictions to be passed back to the network input layer to improve future predictions.

Unlike traditional FFBP ANNs, CPN cannot be over-trained and requires little convergence time. The algorithm was written in MatLab V. 7.4.0.287 (R2007a). For more details refer to Besaw and Rizzo (2007) and Rizzo and Dougherty (1994).

Time-series analysis and ARMAX model

Understanding the temporal relationships between climatic drivers and streamflow is fundamental to the model development. Some studies use time-series correlation analysis to determine the temporal lag (number of time steps) between climate and flow variables (Cigizoglu, 2005b; Kisi, 2005). Similar to Moradkhani et al. (2004), cross-correlation analyses were used in this study to determine the temporal relationships between precipitation, temperature and streamflow.

Autoregressive moving average with exogenous input (ARMAX) is a time-series modeling approach frequently used in the flow forecasting literature for comparison with new flow prediction methods (*e.g.*, Adamowski, 2008). Time-series analysis found the daily streamflow autoregressive and moving average components to be of order 2, while the exogenous variables (precipitation and temperature) were of orders 4 and 1, respectively (Table 2). Thus, the ARMAX model used for comparing daily streamflow predictions is:

$$\hat{Q}(t) = a_1 Q(t-1) + a_2 Q(t-2) + \sum_{i=1}^{4} b_{1i} P(t-i) + b_{21} T(t-1) + c_1 \varepsilon(t-1) + c_2 \varepsilon(t-2),$$

where $Q(t)$ is streamflow at time t, $P(t-i)$ is the precipitation associated with the previous $i = 1,2,\ldots,4$ days, $T(t-1)$ is the average temperature for one day prior, ε is the model error for the previous day (*e.g.*, $\varepsilon(t-1) = \hat{Q}(t-1) - Q(t-1)$). The best fit autoregressive coefficients a_1 and a_2 are associated with the time-lagged streamflow; b_{1i} and b_{21} are the exogenous coefficients associated with precipitation $t-i$ days prior and average temperature one day prior; c_1 and c_2 are the moving average coefficients. The ARMAX model parameters were found using a time-series analysis in the MatLab V. 7.4.0.287 (R2007a) System Identification Toolbox.

Evaluation criteria

Several fundamental metrics are used to evaluate the streamflow forecasting methods (Krause et al., 2005). The root-mean-square error (RMSE) evaluates how closely predictions match observations. Values may range from 0 (perfect fit) to $+\infty$ (no fit) based on the relative range of the data.

The coefficient of determination, r^2, known as the square of the sample correlation coefficient, ranges from 0 to 1 and describes the amount of observed variance explained by the model. A value of 0 implies no correlation, while a value of 1 suggests that the model can explain all of the observed variance.

The Nash–Sutcliffe coefficient of Efficiency, E, measures the model's ability to predict variables different from the mean and gives the proportion of the initial variance accounted for by the model (Nash and Sutcliffe, 1970). It is calculated as:

$$E = 1 - \frac{\sum_{i=1}^{N} (Q_i - \hat{Q}_i)^2}{\sum_{i=1}^{N} (Q_i - \bar{Q})^2},$$

where E ranges from 1 (perfect fit) to $-\infty$. Values less than zero indicate that the observation mean would be a better predictor than the model.

In addition, measures of central tendency and dispersion based on prediction residuals and evaluation of conditional bias are used to evaluate the methods. Mean residuals significantly different from zero often indicate a sub-optimal prediction method.

Model test cases

A total of four test cases are considered in this work (Table 2). The GRNN smoothing parameters (σ^2) were determined through trial-and-error. In all test cases, the CPN and GRNN ANNs used as many hidden nodes as there were training patterns to guarantee one-pass training.

Test case 1

We compare two traditional statistical methods (MLR and ARMAX) with the CPN and GRNN. All of the published MLR and ARMA applications use time-lagged flow *measurements* as model inputs. Although this approach is not suitable to predict flow in ungauged basins, we provide a comparison with these traditional methods using time-lagged measured flow inputs to show that the two proposed ANNs perform as well (or better) than previously published methods when predicting flow using measured flow data. The models predict daily flow for the Dog River and the Winooski River

Table 2
Summary of model implementation details; all models where trained using data from 1996 to 2003 and predicted over the period from 2004 to 2006.

Model test cases	Scale	Training patterns	Prediction patterns	Time-lags			GRNN σ^2
				P	T	Q	
1. Non-recurrent MLR, ARMAX, CPN and GRNN (all seasons)	Daily	2922	1096	4	1	2	0.0052
2. Recurrent CPN and GRNN (summer Qs)	Hourly	30,953	9612	8	24*	2	0.0013
	Daily	1114	381	4	1	2	0.0089
3. Recurrent CPN and GRNN (storm events only)	Hourly	1147	141	8	24*	2	0.0013
	Daily	59	10	4	1	2	0.0089
4. Recurrent CPN and GRNN (summer Qs in an ungauged basin)	Daily	1114	381	4	1	2	0.0089

* Temperature data are available only at the daily time scale.

at Wrightsville. In this test case, *P*, *T* and *measured Q* are used as inputs and flows are forecast for all seasons. Because these predictions use time-lagged *measurements* of streamflow, they provide the most accurate predictive results (as opposed to the remaining test cases that use time-lagged *predictions* of streamflow as inputs).

Test case 2

To explore the recurrent capabilities of the CPN and GRNN, we again forecast streamflow in the Dog River. The purpose is twofold: (1) to explore the predictive capabilities of the recurrent ANNs using time-lagged *predictions* as inputs and (2) to demonstrate the loss of accuracy when using upscaled (*e.g.*, daily) recorded data (as opposed to the raw hourly data) on small streams. We train the recurrent ANNs on summer data from 1996 to 2003 and predict discharge from 2004 to 2006.

Test case 3

We assess the improved performance of the recurrent ANNs when trained on and used to forecast extreme flow events only (*e.g.*, storms or droughts). Specifically, we train the ANNs using nine storm events between 1996 and 2003, and predict using the 2004 data.

Test case 4

The CPN and GRNN were trained on measured climate-flow data from one basin (Dog River) and used to forecast streamflow in another ungauged basin (the Winooski River at Montpelier) using climate data from the weather station nearest Montpelier (Barre/Montpelier Airport). To account for the increase in drainage area from the Dog River (197 km^2) to the Winooski River (1028 km^2), the ANN flow predictions were scaled by the simple ratio of drainage areas: $Q_{winooski} = Q_{dog} * (A_{winooski}/A_{dog})$. This scaling ratio is based on the relationship between bankfull discharge (Q_{bk}) and basin drainage area (A) found by Leopold et al. (1964) to be: $Q_{bk} = eA^f$. Empirical studies show f to vary between 0.7 (semi-arid regions) and 1 (humid landscapes draining small catchments) (Vianello and D'Agostino, 2007). As a result, we use $f = 1$ in Leopold's equation to scale predictions from the smaller to the larger northwestern Vermont basin.

Results and discussion

Data and correlation analysis

Time-series and cross-correlation analyses revealed temporal dependencies between the climate-flow datasets (Fig. 4). The cross-correlation of hourly *P* and *Q* data at increasing time steps found the range of decorrelation to be 8 h (arrow in Fig. 4c). This range of decorrelation represents the maximum time difference at which *P* and *Q* are correlated. After 8 h, these two variables are said to be independent of each other. Observation of the hydrographs and hyetographs confirms a similar time lapse between peak rainfall and peak discharge. A correlation analysis determined a 4-day range of decorrelation for the daily *P*–*Q* data (arrow in Fig. 4d). In addition to *P*–*Q* cross-correlations, *T*–*Q* cross-correlations and *Q*–*Q* auto-correlations determined the temporal range of decorrelation for the remaining model inputs. The results of these analyses are summarized in column 5 of Table 2 (time-lags) and used for all models. It is important to note the difference in time-lags calculated using correlation analysis between the hourly and daily data. Streamflow data, analyzed at the hourly and daily scales, reveal that the upscaling of data to the daily timescale results in the loss of information for these small streams. Fig. 4a and 4b show the hourly and daily Dog River hydrographs and hyetographs for the summer months of 2002. A single storm event occurring in September 2002 highlights the loss of information due to upscaling (Fig. 4e and 4f) in the Winooski watershed, where time-lags between peak storm events and peak discharge are on the order of 8 h to 1 day. Hourly data is needed to sufficiently capture the temporal relationships between measured *P* and instream *Q* for our small streams. It is important to caution users that this is a problem if the driving variables (*e.g.*, climate data) are only available at daily time steps.

Test case 1: daily streamflow comparison of four data-driven methods using gauged discharge

We first compare the four data-driven methods (MLR, ARMAX, CPN and GRNN) to confirm that our coding of the two ANN methodologies produces error metrics and prediction accuracies similar to those published in the literature when using *measured* discharge as a model input. Since measured data are not applicable for our end goal, we later explore predicted discharge as a model input. The four methods use daily time-lagged *P*, *T* and measured *Q* to forecast daily streamflow in two small Vermont sub-basins; the unregulated Dog River and dam-regulated Winooski River at Wrightsville.

We provide measures of comparison between methods in Table 3 and Fig. 5. In the Dog River, the CPN, GRNN and MLR prediction measures of central tendency (median) and dispersion are statistically similar to that of the observed streamflow (Table 3), as determined by the Wilcoxon-rank-sum and Brown-Forsyte tests respectively (type I error rate $\alpha = 0.05$); suggesting these estimation methods are superior to ARMAX in preserving the observed streamflow distribution. The estimated minimum and maximum streamflows suggest that ARMAX over-smoothes the predictions. In addition, MLR and ARMAX predict negative streamflows, an undesirable effect resulting from linear combinations of measured data. The CPN and GRNN residual central tendencies (median) are closer to zero than those of MLR and ARMAX, suggesting that these methods are less globally biased. The prediction scatter plots (Fig. 5) show the CPN predictions to be conditionally biased (*i.e.*, underpredict high flows). Although the error metrics for CPN, GRNN and MLR are statistically similar (*e.g.*, $r^2 = 0.52$, $E = 0.5$ and RMSE = 4.3), they are lower than those typically shown in the literature for these methods (*e.g.*, $r^2 = 0.80$ and $E = 0.80$) (Aytek et al., 2008; Cigizoglu, 2005a). This is likely due to the very rapid hydrological response of this particular basin (*e.g.*, small basin area, narrow shape, steep slopes and thin, impermeable soils), and the loss of accuracy when only upscaled model inputs exist (*e.g.*, averaged daily climate data).

The error metrics calculated for the Winooski River in Wrightsville (Table 3), suggest that all four methods produce statistically similar streamflow estimates and distributions when compared with the measured flow data. None of the error residuals have measures of central tendency statistically different than zero; and the error metrics for these four methods compare well (*e.g.*, $r^2 = 0.79$, $E = 0.78$ and RMSE = 2.7) to those in the literature (Aytek et al., 2008; Cigizoglu, 2005a).

Across both watersheds, the CPN, GRNN and MLR provide the most accurate and unbiased estimators of streamflow. There is no statistical difference in their predictive capability given the selected time-lagged inputs (*P*, *T* and *Q*), suggesting these methods are equally well suited to predict streamflow in the unregulated Dog River and the regulated Winooski River at Wrightsville. All methods produced more accurate predictions in the regulated (less variable flow) Winooski River sub-basin.

Test case 2: streamflow predictions using recurrent CPN and GRNN

Using time-lagged *measurements* of streamflow as model inputs will always result in more accurate predictions than time-lagged

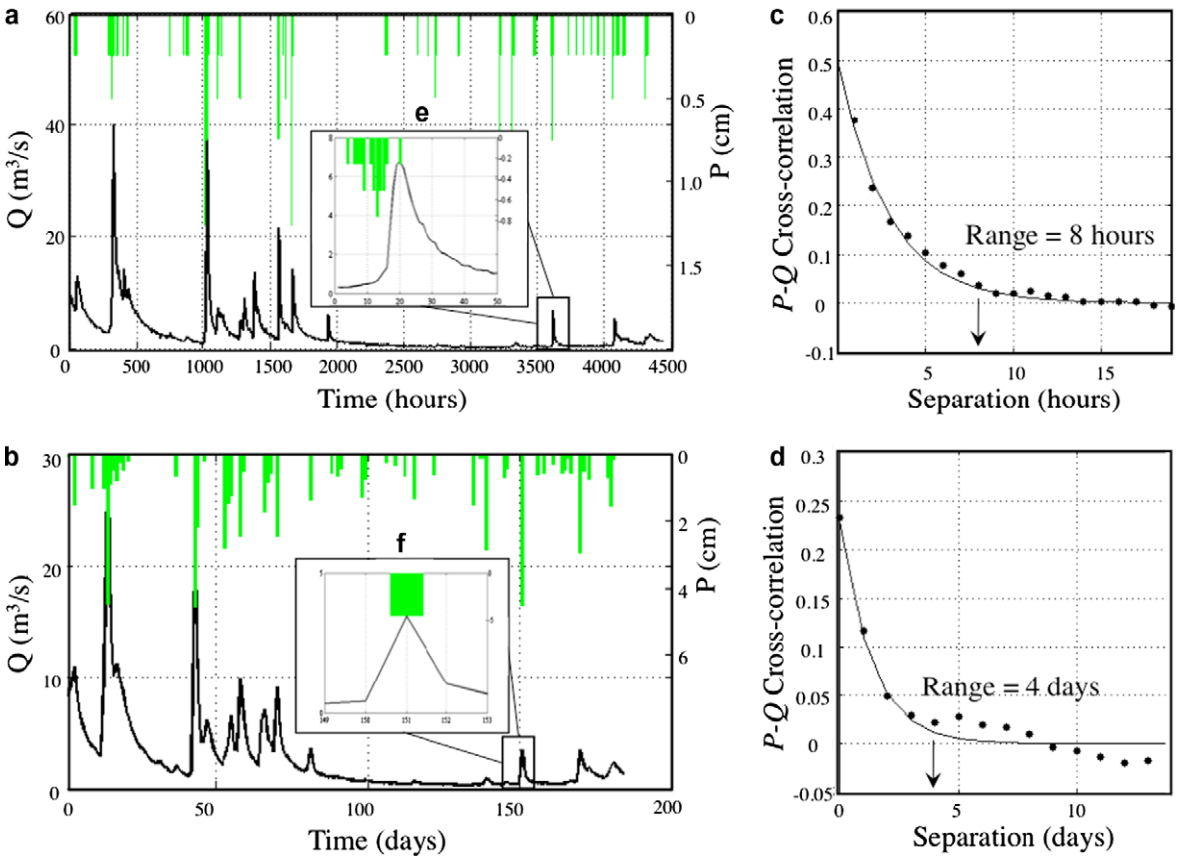

Fig. 4. Dog River hydrograph and hyetograph for the: (a) hourly and (b) daily flow and precipitation records during the summer of 2002. The cross-correlograms (c) and (d) show the temporal relationship (time lag) between *P* and *Q*. Inset showing (e) hourly and (f) daily *Q* and *P* for an individual storm event occurring September 28th.

Table 3
Comparison of measured and predicted streamflow using CPN, GRNN, MLR and ARMAX models in the Dog River and Winooski River at Wrightsville.

	Dog River (m^3/s)					Winooski River at Wrightsville (m^3/s)				
	Q	CPN	GRNN	MLR	ARMAX	*Q*	CPN	GRNN	MLR	ARMAX
Mean	4.8	4.1	4.4	4.6	3.5	5.0	4.8	4.8	4.9	4.7
Median	3.1	2.6	2.7	3.3	2.2	2.8	2.7	2.7	2.9	2.6
Mode	1.0	1.3	1.3	1.7	0.4	0.8	1.0	1.4	1.1	0.7
St. Dev.	6.0	4.4	5.0	4.9	4.8	5.8	5.2	5.1	5.2	5.6
Min	0.4	0.4	1.0	−1.1	−2.1	0.23	0.3	0.6	0.0	0.0
Max	71	55	53	61	46	25.4	24.6	26.5	25.8	26.0
R^2	1	0.53	0.51	0.51	0.42	1	0.80	0.77	0.79	0.79
E	1	0.51	0.49	0.50	0.36	1	0.80	0.77	0.80	0.78
RMSE	0	4.2	4.3	4.3	4.8	0	2.6	2.8	2.6	2.7
R. Mean	0	−0.7	−0.4	−0.2	−1.3	0	−0.3	−0.2	−0.1	−0.3
R. Median	0	−0.1	0.1	0.4	−0.7	0	0.1	0.3	0.3	−0.1
R. St. Dev.	0	4.2	4.3	4.3	4.7	0	2.6	2.8	2.6	2.7

estimates of streamflow. Thus, we expect error metrics worse than those published in the literature (and shown in Test case 1). However, using predicted (rather than observed) flow moves us one step closer to providing forecasts at nearby basins and/or other locations within the river network (*e.g.*, ungauged basins). When using the recurrent ANNs for prediction, the algorithm must provide an initial value (or best guess) of streamflow at $t = 0$. In this work, we initialize flow with either an observed value or an estimate of baseflow. Both proved equally successful, primarily because the measured climate data drive the ANN streamflow predictions.

The recurrent CPN and recurrent GRNN are used to predict hourly and daily streamflow for the summer months from 2004 to 2006. Fig. 6 presents a subset of the data (a 90-day window in the summer of 2004) to show time-series predictions without compromising the figure legibility. Both recurrent ANNs capture the streamflow trends within this time frame. However, there are noticeable differences between the two timescales.

Error metrics at the hourly and daily timescales (Table 4) show the hourly models to be superior. As expected, both ANNs better capture the climate-flow relationships when trained on the hourly data (r^2 of 0.45 vs. 0.29) reflecting the basin-scale characteristics. The Dog River basin has a very flashy response to precipitation events. This flashiness is a function of specific basin characteristics (*e.g.*, small basin area, narrow shape, steep slopes and thin, impermeable soils).

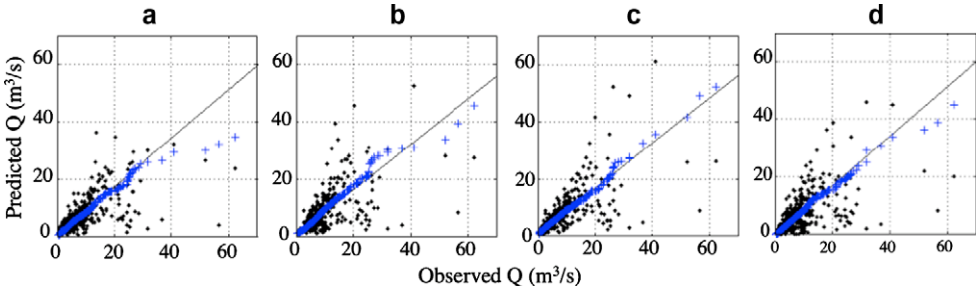

Fig. 5. Comparison of measured and predicted streamflow using: (a) CPN, (b) GRNN, (c) MLR and (d) ARMAX models in the Dog River against theoretical quantile line. Flow quantiles shown as (+).

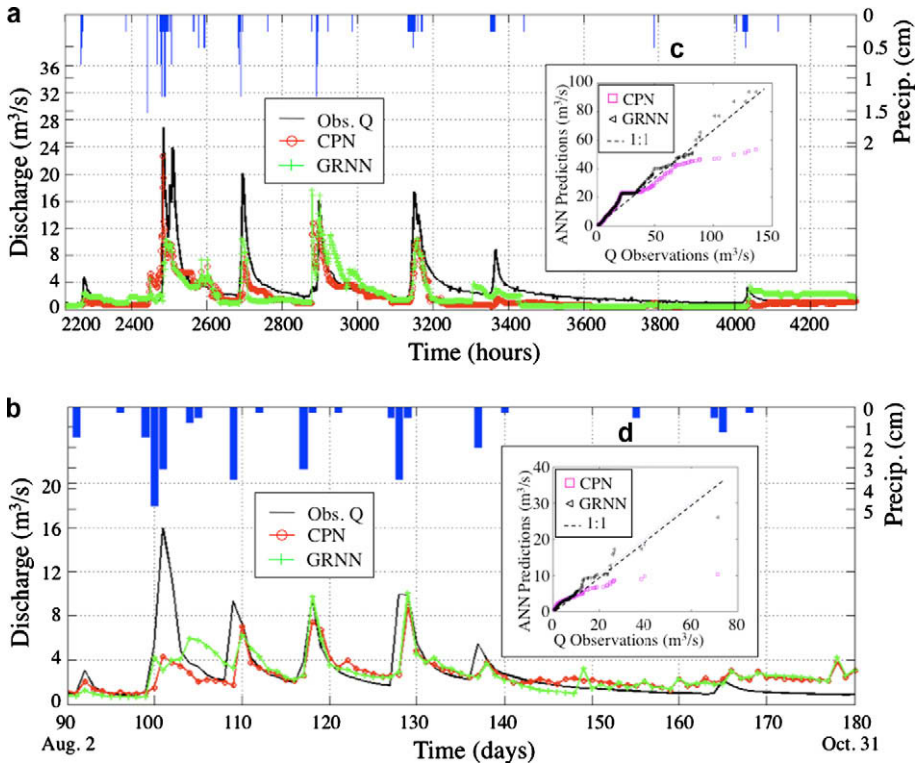

Fig. 6. Time-series streamflow observations and ANN predictions at the: (a) hourly and (b) daily timescales for a 90-day window of summer 2004 using two recurrent ANNs. The inset figures represent the *qq*-plots for all summer forecasts 2004–2006 at (c) hourly and (d) daily timescales.

Table 4
Hourly and daily error metrics for the CPN and GRNN summer flow predictions at the Dog River from 2004 to 2006.

	CPN		GRNN	
	Daily	Hourly	Daily	Hourly
R^2	0.29	0.5	0.29	0.45
E	0.16	0.28	0.02	0.28
RMSE	5.5	5.2	5.9	5.5
Corr	0.53	0.7	0.53	0.67
n	381	9612	381	9612

The upscaling of hourly data to the daily scale reduces the accuracy of the ANN streamflow forecasts. This is evidenced by the shift in peak flow estimates (Fig. 6b). Different characteristic time-lags between P and Q were identified using time-series analysis for the daily and hourly flow – 8 h and 4 days respectively (Fig. 4c and d). Eight hours was also the typical time lag observed when plotting the peak rainfall and peak storm flow events. Thus, the daily data are not capturing the 8-h temporal relationship between P and Q; and upscaling the hourly data to the daily scale results in a loss of prediction accuracy for both ANNs.

As on might expect, the prediction errors increase when compared to predictions using measured flow as inputs (*e.g.*, r^2 and E values of 0.5 and 0.28). Coefficients of determination and efficiency calculated for the Dog River decrease from 0.53 to 0.29 and from 0.51 to 0.16 respectively; while RMSE increases from 4.2 to 5.2. However, the use of recurrent feedback with estimated flow is necessary to develop methods capable of forecasting flows in ungauged basins. Whether these forecasts are "accurate" enough, however, depends on the user's application.

Both the GRNN and, to a greater extent, the CPN predictions contain conditional bias in that they tend to underpredict high flows (Fig. 6c and d). These *qq*-plots compare distributions of $\hat{Q}$ and Q for each ANN at each time scale. Such bias is expected (Chang and Chen, 2001; Firat, 2008), as the majority of recorded data (both training and prediction) consist of base flow events. As a result, it is common in the ANN literature to improve forecasts by creating specialized ANNs (and associated training datasets)

that separately predict low and high flows (Rajurkar et al., 2002; Singh and Deo, 2007).

Test case 3: extreme-event streamflow predictions using recurrent CPN and GRNN

As a proof-of-concept, we re-trained the recurrent ANNs of Test case 2 on nine storm events from the summer months of 1996–2003. A comparison of the error metrics for these two specialized storm flow-event ANNs shows much improvement (Table 5) over the ANNs used to predict both high and low flows (Table 4) at both timescales. The measurements and predictions of a single storm event (October 2004) is shown in Fig. 7 to legibly demonstrate the information lost due to unscaling hourly data to the daily timescale.

As with all data-driven methods, ANN predictions are only as good as the data on which they were trained. Both ANN models show greater prediction accuracies using hourly data, further highlighting the importance of measurement scale. The methods presented here require training on some known (observed) set of climate-flow data. In addition, the stationarity assumption must hold. A good example in this work is the assumption that general landuse patterns do not change. If the basin of interest has undergone extensive landuse changes, climate-flow data used for training the ANN may not be appropriate for the time period in which predictions are needed. Through an analysis of historical aerial photographs, (Hackett, 2009) documented the changes in land cover and subsequent changes in basin discharge. This was our motivation for selecting a 10 year subset of the 70 year Winooski Basin dataset to train and test our methods.

Test case 4: predicting streamflow in ungauged basins

The recurrent CPN and GRNN models, trained using climate-flow data from the Dog River, were used to predict streamflow in the nearby Winooski River at Montpelier for the summer months from 2004 to 2006; but only a 90-day window in 2004 is displayed (Fig. 8). Both ANNs predict the general streamflow trends in response to climate drivers. The climate-flow record from the Northfield NCDC weather station was used to train the ANNs, while the climate record from the Barre/Montpelier Airport weather station was used for making predictions. Cigizoglu (2003) and Kisi (2008) have also shown that it is possible to train on one watershed and predict on another. However, they used measured flow as an input, while here we have used estimated flow in combination with recurrent feedback connections in the CPN and GRNN.

Table 5
Storm prediction hourly and daily error metrics for CPN and GRNN predictions at the Dog River.

	CPN		GRNN	
	Daily	Hourly	Daily	Hourly
R^2	0.75	0.87	0.75	0.95
E	0.74	0.52	0.58	0.74
RMSE	2.20	3.81	2.81	2.82
Corr	0.87	0.93	0.87	0.97
n	10	141	10	141

The qq-plot of predicted and observed Q (Fig. 8b), shows the method to scale well over a wide range of flows (between 1 and 90 m^3/s). This is encouraging given the simplicity of the scaling algorithm across different watersheds. Predicted flows were upscaled by the ratio of drainage areas, suggesting this method sufficiently accounts for the increase in streamflow in the larger basin. However, the ANNs overpredict measured flows greater than 90 m^3/s (discharge plot above the theoretical quantile line). Two potential solutions exist to correct for this conditional bias. The first is to once again train the ANNs only on extreme events (*e.g.*, create separate high and low flow ANNs). The second is to use a coefficient of f less than 1 in the Leopold equation for flows above the 90 m^3/s threshold. For this particular test case, the ANNs were trained on the climate-flow relationships from the smaller sub-basin and predictions were scaled up to a larger sub-basin; but the ANNs could just as easily be trained on paired climate-flow data from a larger sub-basin and predictions scaled down to a smaller sub-basin.

For several storm events of Fig. 8, the predicted $\hat{Q}$ lags behind the observed Q. This is again due to the loss of information in upscaling the hourly data to the daily timescale. Predictions would be improved if the climate-flow relationships were better captured in the data (*e.g.*, hourly data).

Error metrics calculated over the three forecasting years (Table 6) indicate the CPN outperforms the GRNN. Errors would have been less had hourly data been used. There are benefits of the GRNN model: it is a single-pass training algorithm and does not require the functional form of the regression line be specified *a priori*. One disadvantage is that the GRNN does not perform well with irrelevant inputs without major modification of Specht's original algorithm. Therefore, it is not a good choice with more than 5 or 6 non-redundant inputs. The CPN algorithm used in this work does not require iterative training, while the GRNN smoothing parameter, σ^2, must be iteratively optimized through trial-and-error. The greater accuracy (Table 6) makes the CPN a slightly more suitable method this for particular application – predicting streamflow in ungauged basins.

The transfer of the CPN methodology from one basin to another, and subsequent scaling of predicted flows by the ratio of drainage

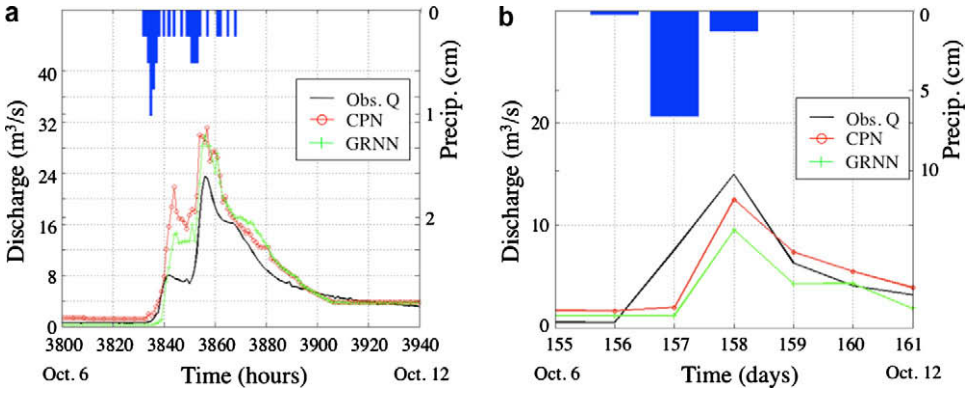

Fig. 7. CPN and GRNN streamflow predictions trained only on storm events at the: (a) hourly and (b) daily timescales.

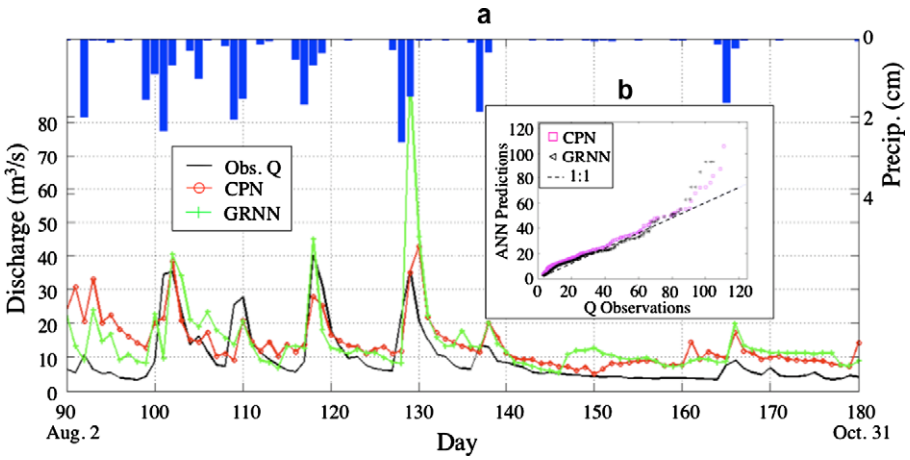

Fig. 8. Time-series streamflow observations and ANN predictions on the Winooski River at Montpelier: (a) over a 90 day forecast period (summer of 2004) and (b) *qq*-plots for three summer prediction periods (2004–2006) using recurrent ANNs trained on the Dog River.

Table 6
Error metrics for the Winooski River at Montpelier flow predictions from 2004 to 2006.

	CPN	GRNN
R^2	0.24	0.16
E	0.12	−0.35
RMSE	18.0	22.7
Corr	0.49	0.37
n	540	540

areas, does not result in a significant loss of prediction. This is contingent on the basins having similar geological and geographical characteristics (*e.g.*, shape, slopes, soils) as well as landuse patterns. These basins were primarily forested (83% in Winooski and 85% in Dog sub-basins, respectfully) with marginal impermeable (5% and 8%) and cleared (12% and 7%) landuse types (Hackett, 2009). Training the CPN on daily data from the Dog River and predicting in the same sub-basin resulted in a CPN r^2 of 0.29, while training on the Dog River and predicting flow on the Winooski River at Montpelier resulted in a CPN r^2 of 0.24; and whether these forecasts are "accurate" enough depends on the user's application. The successful transference of the models from one basin to another is primarily a function of: (1) using measured local climate data as the driver (inputs) and (2) training the network on a sufficiently large number of regional climate-flow data (*e.g.*, flood and low flow events) over a time period when landuse did not change significantly.

Conclusions

Two recurrent ANN models were trained on climate-flow data from one basin and used to make predictions with climate data from another nearby basin. The recurrent counterpropagation network (CPN) forecasts daily streamflow in the nearby, ungauged basins as accurately as in the basin on which it was trained. One of the key results of this work, and the reason why time-lagged predictions of steamflow improve forecasts, is that the recurrent flow predictions (used as model inputs) are driven by time-lagged locally-measured climate data. Climate data are driving the system. This is also the reason that the models are relatively insensitive to our initial guess of streamflow. A simple ratio, based on a relationship between bankfull discharge and basin drainage area, was used to scale flow predictions between basins with different drainage areas.

The two recurrent ANN models were first compared with other traditional data-driven methods using time-lagged *measured* flow data as model inputs. Error metrics show flow predictions to be similar to those in the published literature. Using time-lagged flow observations as inputs, as opposed to time-lagged predictions, does produce more accurate results; however, this approach is not applicable in ungauged basins. As a result, we focus on recurrent methods of using time-lagged predictions of flow and measured climate data as model inputs.

Basin characteristics (*e.g.*, shape, slope) had an important effect on model accuracies at different temporal scales. In this case, predictions using hourly data were more accurate than those using daily data because important climate-flow relationships were lost when using the upscaled daily data. Time-series analysis of the climate-flow data provided a transferable and systematic methodology for determining appropriate number of time-lagged model inputs. The successful demonstration of these flow prediction methods with publically available USGS flow and NCDC climate datasets suggests the proposed methods are applicable in humid, temperate climate zones.

By selecting data-driven ANNs that always converge and avoid stochastic training, these methodologies are straightforward to execute and widely applicable to small ungauged basins. As such, they should prove useful to watershed and water resources management stakeholders.

Acknowledgements

This research was supported in part by the United States Department of Transportation through the University of Vermont Transportation Research Center, the National Science Foundation VT EPSCoR Grant (NSF EPS #0701410), the US Geological Survey, and the Vermont Agency of Natural Resources and is a contribution from the Water Resources and Lake Studies Center. The findings, conclusions, recommendations and opinions stated in this report are those of the authors and do not represent the views of these funding agencies.

References

Adamowski, J.F., 2008. Development of a short-term river flood forecasting method for snowmelt driven floods based on wavelet and cross-wavelet analysis. Journal of Hydrology 353, 247–266.
Albers, J., 2000. Hands on the Land. A History of the Vermont Landscape. MIT Press, Cambridge, MA.
Allen, J.D., 1995. Stream Ecology: Structure and Function of Running Waters. Springer, Dordrecht, Neth. 388 pp.

Alp, M., Cigizoglu, H.K., 2007. Suspended sediment load simulation by two artificial neural network methods using hydrometeorological data. Environmental Modeling & software 22, 2–13.
Arnell, N., et al., 2001. Climate change 2001: impacts, adaptation and vulnerability: hydrology and water resources. United Nations Environmental Program, Intergovernmental Panel on Climate Change.
Aytek, A., Asce, M., Alp, M., 2008. An application of artificial intelligence for rainfall–runoff modeling. Journal of Earth System Science 117 (2), 145–155.
Besaw, L.E., Rizzo, D.M., 2007. Stochastic simulation and spatial estimation with multiple data types using artificial neural networks. Water Resources Research 43, W11409. doi:10.1029/2006WR005509.
Brooks, K.N., Ffolliott, P.F., Gregersen, H.M., DeBani, L.F., 2003. Hydrology and the Management of Watersheds. Iowa State Press, Ames, IA.
Chaloulakou, A., Assimacopoulos, D., Lekkas, T., 1999. Forecasting daily maximum ozone concentration in the Athens basin. Environmental Monitoring and Assessment 56 (97–112).
Chang, F.J., Chen, Y.-C., 2001. A counterpropagation fuzzy-neural network modeling approach to real time stream flow prediction. Journal of Hydrology 245, 153–164.
Chang, F.J., Hu, H.F., Chen, Y.C., 2001. Counterpropagation fuzzy-neural network for streamflow reconstruction. Hydrological Processes 15 (2), 219–232.
Chang, F.J., Chang, L.C., Huang, H.-L., 2002. Real-time recurrent learning neural network for stream-flow forecasting. Hydrological Processes 16, 2577–2588.
Chiew, F., McMahon, T., 1994. Application of the daily rainfall runoff model MODHYDROLOG to 28 catchments. Journal of Hydrology 153 (1–4), 383–416.
Cigizoglu, H.K., 2003. Estimation, forecasting and extrapolation of river flows by artificial neural networks. Hydrological Sciences 48 (3), 349–361.
Cigizoglu, H.K., 2005a. Application of generalized regression neural networks to intermittent flow forecasting and estimation. Journal of Hydrologic Engineering 10 (4), 336–341.
Cigizoglu, H.K., 2005b. Generalized regression neural network in monthly flow forecasting. Civil Engineering and Environmental Systems 22 (2), 71–84.
Connor, J.T., Martin, R.D., Atlas, R.D., 1994. Recurrent neural networks and robust time series prediction. IEEE Transactions on Neural Networks 5 (2), 240–254.
Doolan, B., 1996. The Geology of Vermont. Rocks and Minerals 71, 218–225.
Emrah, D., Yuksel, I., Kisi, O., 2007. Estimation of total sediment load concentration obtained by experimental study using artificial neural networks. Environmental fluid mechanics 7 (4), 271–288.
Firat, M., 2008. Comparison of artificial intelligence techniques for river flow forecasting. Hydrology and Earth System Sciences 12, 123–139.
Firat, M., Gungor, M., 2008. Hydrological time-series modelling using an adaptive neuro-fuzzy inference system. Hydrological Processes 22, 2122–2132.
Geological_Survey, US, 2009. USGS Surface-Water Data for USA.
Govindaraju, R.S., 2000. Artificial neural networks in hydrology II: hydrogeologic applications. Journal of Hydrologic Engineering 5 (2), 124–137.
Govindaraju, R.S., Ramachandra, R.A., 2000. Artificial Neural Networks in Hydrology. Kluwer Academic Publishers, Dordrecht, The Netherlands.
Hackett, W.R., 2009. Changing Land Use, Climate and Hydrology in the Winooski River Basin, Vermont. M.S. Thesis, Univ. of Vermont, Burlington.
Hecht-Nielsen, R., 1987. Counterpropagation Networks. Applied Optics 26 (23), 4979–4984.
Hijmans, R.J., Cameron, S.E., Parra, J.L., Jones, P.G., Jarvis, A., 2005. Very high resolution interpolated climate surface for global land areas. International Journal of Climatology 25, 1965–1978.
Hsieh, W.W., Yuval, L.J.Y., Shabbar, A., Smith, S., 2003. Seasonal prediction with error estimation of Columbia river streamflow in British Columbia. Journal of Water Resources Planning and Management – ASCE 129 (2), 146–149.
Hsu, K., Gupta, H.V., Sorooshian, S., 1995. Artificial neural network modeling of the rainfall–runoff process. Water Resources Research 31 (10), 2517–2530.
Hsu, K.L., Gupta, H.V., Sorooshian, G.S., Imam, B., 2002. Self-organizing linear output map (SOLO): an artificial neural network suitable for hydrologic modeling and analysis. Water Resources Research 38 (12), 1312. doi:10.1029/2001WR001118.
Jakeman, J.J., Littlewood, I.G., Whitehead, P.G., 1990. Computation of the instantaneous unit hydrograph and identifiable component flows with application to two small upland catchments. Journal of Hydrology 117, 275–300.
Khalil, A.F., McKee, M., Kemblowski, M., Asefa, T., 2005. Basin scale water management and forecasting using artificial neural networks. Journal of American Water Resources Association 41 (1), 195–208.
Kingston, G.B., Maier, H.R., Lambert, M.F., 2005. Calibration and validation of neural networks to ensure physically plausible hydrological modeling. Journal of Hydrology 314, 158–176.
Kisi, O., 2005. Daily river flow forecasting using artificial neural networks and auto-regressive models. Turkish Journal of Engineering and Environmental Sciences 29 (1), 9–20.
Kisi, O., 2008. River flow forecasting and estimation using different artificial neural network techniques. Hydrology Research 39 (1), 27–40.
Kokkonen, T.S., Jakeman, A.J., 2001. A comparison of metric and conceptual approaches in rainfall–runoff modeling and its implications. Water Resources Research 37 (9), 2345–2353.
Krause, P., Boyle, D.P., Base, F., 2005. Comparison of different efficiency criteria for hydrological model assessment. Advances in Geosciences 5, 89–97.
Leopold, L.B., Wolman, M.G., Miller, J.P., 1964. Fluvial Processes in Geomorphology. Freeman, San Francisco. 522 pp.
Maier, H.R., Dandy, G.C., 2000. Neural networks for the prediction and forecasting of water resources variables: a review of modelling issues and applications. Environmental Modelling & Software 15, 101–124.
McKerchar, A.I., Delleur, J.W., 1974. Applications of seasonal parametric linear stochastic models to monthly flow data. Water Resources Research 10, 246–255.
Mohamoud, Y.M., 2008. Prediction of daily flow duration curves and streamflow for ungauged catchments using regional flow duration curves. Hydrological Sciences 53 (4), 706–724.
Moradkhani, H., Hsu, K.-L., Gupta, H.V., Sorooshian, S., 2004. Improved streamflow forecasting using self-organizing radial basis function artificial neural networks. Journal of Hydrology 295, 246–262.
Nash, J.E., Sutcliffe, J.V., 1970. River flow forecasting through conceptual models, Part I – a discussion of principles. Journal of Hydrology 10, 282–290.
Phien, H.N., Huong, B.K., Loi, P.D., 1990. Daily forecasting with regression analysis. Water SA 16 (3), 179–184.
Rajaee, T., Mirbagheri, S.A., Zounemat-Kermani, M., Nourani, V., 2009. Daily suspended sediment concentration simulation using ANN and neuro-fuzzy models. Science of the total environment 407, 4916–4927.
Rajurkar, M.P., Kothyari, U.C., Chaube, U.C., 2002. Artificial neural networks for daily rainfall–runoff modelling. Hydrological Sciences 47 (6), 865–877.
Rizzo, D.M., Dougherty, D.E., 1994. Characterization of aquifer properties using artificial neural networks: neural kriging. Water Resources Research 30 (2), 483–497.
Schilling, K.E., Wolter, C.F., 2005. Estimation of streamflow, baseflow and nitrate–nitrogen loads in Iowa using multiple regression models. Journal of American Water Resources Association 41 (6), 1333–1346.
Singh, P., Deo, M.C., 2007. Suitability of different neural networks in daily flow forecasting. Applied Soft Computing 7, 968–978.
Specht, D.F., 1991. A general regression neural network. IEEE Transactions on Neural Networks 2 (6).
Tangborn, W.V., Rasmussen, L.A., 1976. Hydrology of the North Cascades region, Washington – Part 2: a proposed hydrometeorological streamflow prediction method. Water Resources Research 12, 203–216.
VanderKwaak, J.E., Loague, K., 2001. Hydrologic-response simulations for the R-5 catchment with a comprehensive physics-based model. Water Resources Research 37 (4), 999.
Vianello, A., D'Agostino, V., 2007. Bankfull width and morphological units in an alpine stream of dolomites (Northern Italy). Geomorphology 83, 266–681.
Walker, J.P., Houser, P.R., Reichle, R.H., 2003. New technologies require advances in hydrologic data assimilation. EOS 84, 545–551.
Wang, W., Van-Gelder, P.H.A.J.M., Vrijling, J.K., Ma, J., 2006. Forecasting daily streamflow using hybrid ANN models. Journal of Hydrology 324, 383–399.
Wang, Y.-C., Chen, S.-T., Yu, P.-S., Yang, T.-C., 2008. Storm-even rainfall–runoff modelling approach for ungauged sites in Taiwan. Hydrological Processes 22, 4322–4330.
Yang, M.-D., Chen, B.P.T., Chen, C.-S., 2007. Using artificial neural network for outflow estimation in an ungauged area. In: IEEE International Joint Conference on Neural Networks, pp. 3551–3555.
Yurekli, K., Kurung, A., Ozturk, F., 2005. Testing residuals of an ARIMA model on the Cekerek stream watershed in Turkey. Turkish Journal of Engineering and Environmental Sciences 29, 61–74.
Zealand, C.M., Burn, D.H., Simonovic, S.P., 1999. Short term streamflow forecasting using artificial neural networks. Journal of Hydrology 214, 32–48.